Research Paper

MMP-9 overexpression is associated with intragenic hypermethylation of MMP9 gene in melanoma

Luca Falzone[1], Rossella Salemi[1], Salvatore Travali[1], Aurora Scalisi[2], James A. McCubrey[3], Saverio Candido[1*], and Massimo Libra[1*]

[1]Department of Biomedical and Biotechnological Sciences, Laboratory of Translational Oncology & Functional Genomics, Section of General & Clinical Pathology and Oncology, University of Catania, 95124, Catania, Italy
[2]Oncological Pathology Unit, ASP, Catania, Italy;
[3]Department of Microbiology and Immunology, Brody School of Medicine, East Carolina University, Greenville, NC 27858, USA
**Co-last authors*

Key words: *MMP-9, epigenetic, intragenic, methylation, melanoma*
Received: *03/16/16; Accepted: 04/19/16; Published: 04/25/16*
Correspondence to: *Massimo Libra, MD/PhD; Saverio Candido, PhD;* ***E-mail:*** *mlibra@unict.it; scandido@unict.it*

Abstract: Tumor spreading is associated with the degradation of extracellular matrix proteins, mediated by the overexpression of matrix metalloproteinase 9 (MMP-9). Although, such overexpression was linked to epigenetic promoter methylation, the role of intragenic methylation was not clarified yet. Melanoma was used as tumor model to investigate the relationship between the DNA intragenic methylation of *MMP9* gene and MMP-9 overexpression at transcriptional and protein levels. Computational analysis revealed DNA hypermethylation within the intragenic CpG-2 region of *MMP9* gene in melanoma samples with high MMP-9 transcript levels. In vitro validation showed that CpG-2 hotspot region was hypermethylated in the A375 melanoma cell line with highest mRNA and protein levels of MMP-9, while low methylation levels were observed in the MEWO cell line where MMP-9 was undetectable. Concordant results were demonstrated in both A2058 and M14 cell lines. This correlation may give further insights on the role of *MMP-9* upregulation in melanoma.

INTRODUCTION

Metastatic spreading is the major cause of death in tumor patients [1,2]. Several molecules have been shown to contribute to tumor invasion and spreading. Among these, matrix metalloproteinase 9 (MMP-9) overexpression has been associated with tumor dissemination [3]. This evidence suggests its role as a prognostic factor.

However, the increased levels of MMP-9 have been described in several pathologic conditions and/or inflammatory status suggesting that it is not clearly specific in cancer [4]. Accordingly, several inflammatory cytokines and growth factors that in turn may activate the Activator Protein-1/A Polyoma Enhancer Binding Protein-3 factor (AP-1/PEA3) and NF-kB led MMP-9 overexpression [5,6]. Constitutive increased expression of MMP-9 may be determined by genetic modifications such as polymorphisms. Among these, the C-1562T polymorphism, upstream to the start site of transcription, and the alteration of di-nucleotide CA repeats in the AP-1 regulatory sequence, were more frequent [7].

Further mechanisms of gene modulation have been associated with epigenetic modifications. In particular, the overexpression of different genes was related to the hypomethylation of gene promoter through chromatin decondensation, allowing the recruitment of the transcriptional complex. Moreover, demethylation of consensus sequence of transcription factors lets the

binding of these transcription factors with promoter regions resulting in the gene upregulation, including that of *MMP9* [8,9,10].

Most recently, it was demonstrated that intragenic DNA methylation could affect the gene expression [10]. The authors reported that the intragenic methylation is positively correlated with the expression of the same gene and negatively correlated with the majority of histone modifications. In particular, it was speculated that intragenic methylation might have roles in the mechanisms of transcriptional elongation, intragenic activation (enhancer) and alternative splicing [10].

According to these evidences, the analysis of cancer epigenetic modifications is the best approach to discriminate if MMP-9 overexpression is directly associated with tumor progression and not with co-morbidities or inflammatory status. Therefore, in the present study we performed in silico and in vitro analyses to assess the methylation patterns of *MMP9* gene in melanoma and its implication in MMP-9 mRNA overexpression [11]. The choice of this tumor type was based on its highly invasive and metastatic characteristics where MMP-9 overexpression may play an important role [3].

RESULTS

Computational identification of an intragenic methylation hotspot in the *MMP9* gene

Four CpG islands were identified within the *MMP9* locus using the bioinformatic tool CpG Islands Tracks available in UCSC Genome browser (https://genome-euro.ucsc.edu). These regions were named CpG-1, CpG-2, CpG-3, CpG-4 according to their relative position in the *MMP9* sequence (Figure 1A, Table S1). In addition, the methylation analysis of *MMP9* gene was performed comparing 6 normal cell lines with 7 cancer cell lines using the bioinformatic ENCODE DNA Methylation RRBS (Figure 1B). As reported in the Figure 1B, the cancer cell lines showed a hypermethylated region (red and yellow bars) inside the annotated CpG-2 island compared to the normal cell lines (green bars). This region, located at chromosomal position CH20:46012338-46012584 (GRCh38 Primary Assembly), was reported in this study as a CpG-2 hotspot region.

MMP-9 correlated levels of intragenic hypermethylation and mRNA expression in melanoma: computational analysis

The transcript levels of *MMP9* in the samples analyzed in GSE31879 melanoma dataset were about 1.5 fold higher in melanoma samples compared to melanocyte controls ($p<0.01$) (Figure S1A). Afterwards, we proceeded to stratify melanoma samples into low (below 30th percentile), medium (between 30th and 70th percentile) and high (above 70th percentile) groups according to the levels of MMP-9 mRNA expression. Statistical analysis revealed that in the high and medium groups, MMP-9 levels were significantly overexpressed as compared to both the low group and melanocytes ($p<0.01$) (Figure S1B). Furthermore, Pearson correlation analysis was performed between MMP-9 expression levels and methylation intensity of *MMP9*-

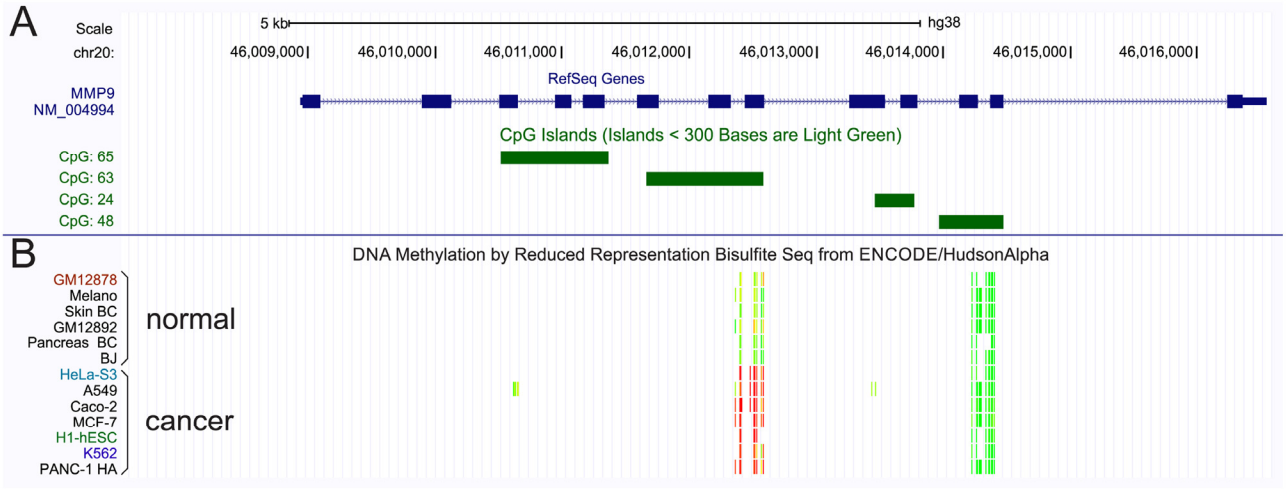

Figure 1. MMP9 methylation pattern. (**A**) Computational detection of CpG islands within the MMP9 locus. (**B**) Methylation status of MMP9 gene, performed by ENCODE RRBS tool, in 6 normal cells compared to 7 cancer cells.

specific probes in selected samples included in GSE31879 dataset. The statistical analysis reveals a moderate positive correlation ($p<0.05$) between MMP-9 levels and methylation status of probes belonging to CpG-2 group (Figure 2, Table S2). When the melanoma samples were stratified in high, moderate and low group according the levels of MMP-9 expression, the CpG-2 region was hypermethylated in the MMP-9 high-expression melanoma samples (box 4) compared to other groups, including melanocyte controls (box 1-3) (Figure 3A). The cumulative statistical analysis of methylation levels of *MMP9* showed a significant difference among the four groups in CpG-2 region ($p<0.01$); while, in GpG-1 island statistical significance difference was observed only for high vs medium ($p<0.01$) and high vs low ($p<0.05$) (Figure 3B).

Positive correlation between MMP-9 expression and hyper-methylation of CpG-2 hotspot in melanoma cell lines

Protein and mRNA levels of MMP-9 were tested in A375, A2058, M14 and MEWO melanoma cell lines by ELISA test and RT-qPCR, respectively. Real-time analysis revealed that *MMP-9* gene expression was 100-fold higher in A375 compared to other cell lines (Figure 4A). Similar results were obtained by ELISA. Soluble MMP-9 levels were 2024.6 pg/mL for A375 and 13.2 pg/mL for A2580, whereas M14 and MEWO cell lines showed MMP-9 protein levels undetectable by the ELISA kit used in this study (Figure 4B).

Methylation status of *MMP9* at CpG-2 hotspot sequence, as identified by computational approach, was analyzed using the methylation-specific restriction enzyme (MSRE) assay. This was performed as a one-step protocol using the methylation-sensitive HpaII restriction enzyme, that is able to digest the unmethylated DNA but not methylated at 5'-CCGG-3'sites. Digested DNA and non-digested DNA (control reference), of each melanoma cell line samples were subjected to q-PCR to amplify the putative CpG-2 hotspot region, containing 6 HpaII consensus sites.

As expected, higher amplification levels of CpG-2 hotspot sequence were observed in A375 compared to other cell lines. A2058 and M14 showed lower relative methylation levels (< 50%) compared to those observed in A375. While, no amplification signal was observed in the MEWO cell line (Figure 4C).

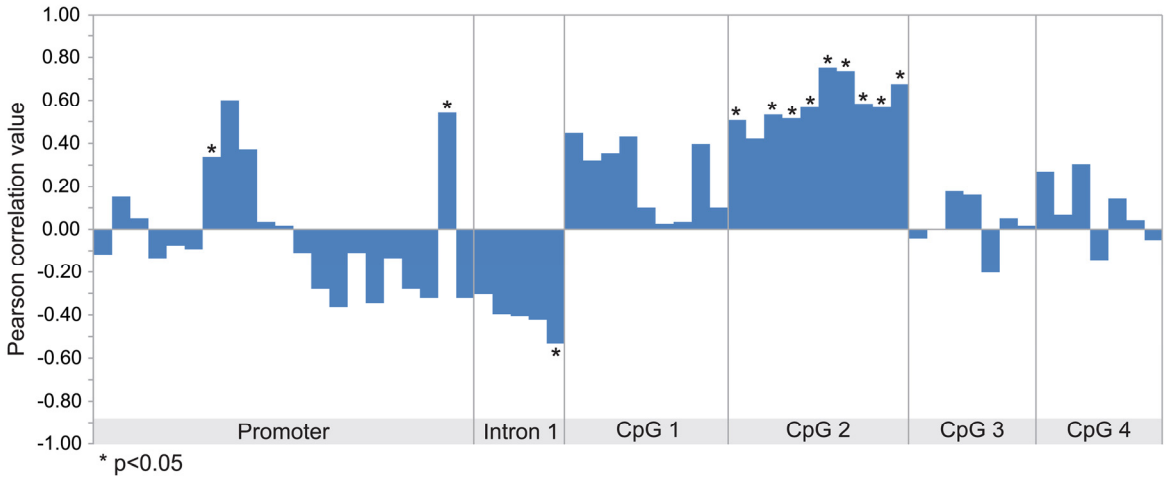

Figure 2. Correlation between MMP-9 expression and methylation status of MMP9 gene. Pearson correlation analysis between methylation levels of each probeset and MMP-9 expression performed in all samples included in GSE31879 dataset.

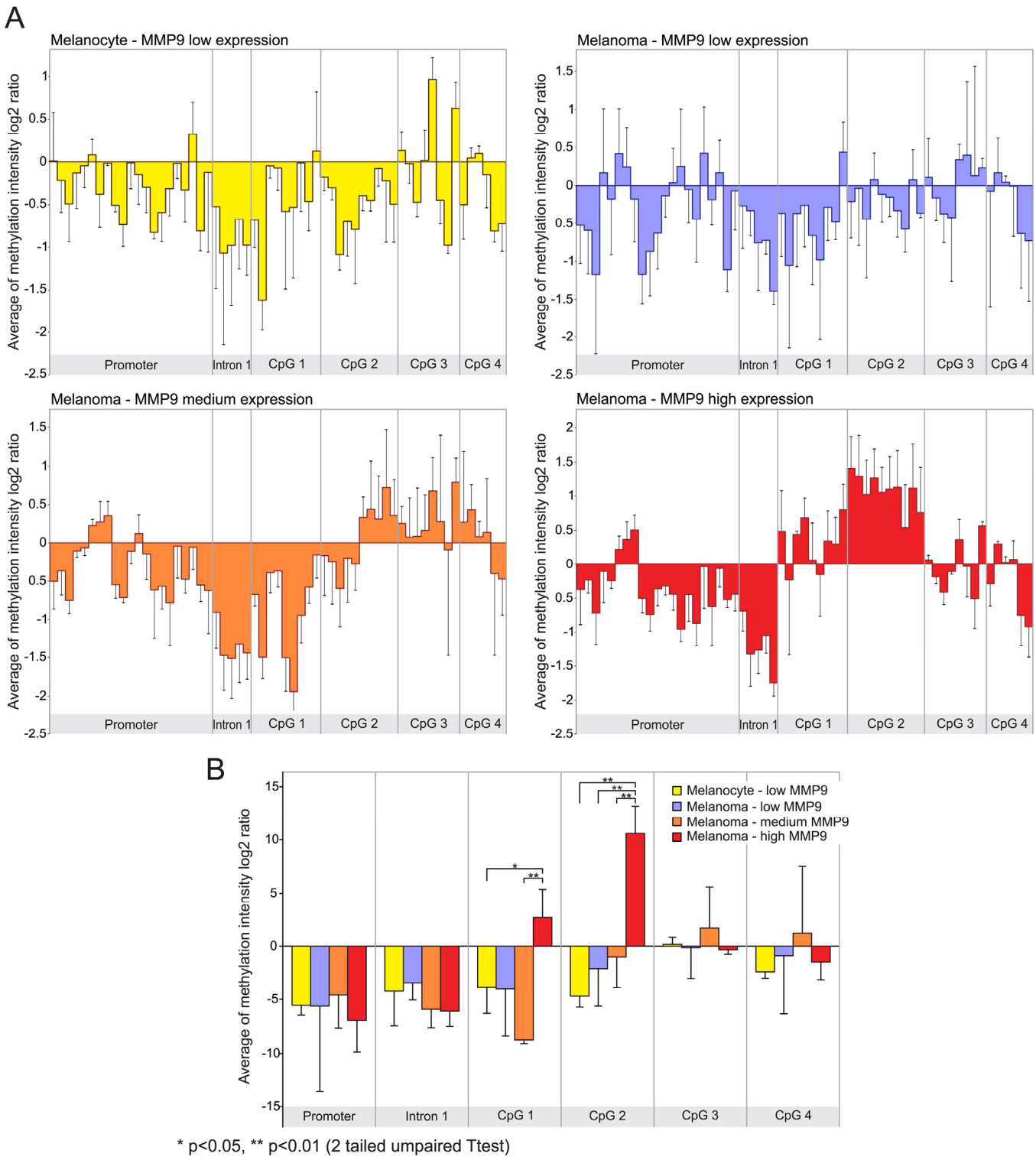

Figure 3. Differential analysis of MMP-9 expression and methylation status of MMP9 gene according to MMP-9 expression levels. (**A**) Methylation analysis of MMP9 locus in the MMP-9 expression groups of melanoma samples, and melanocyte controls. (**B**) Cumulative statistical analysis of methylation levels of MMP9 in stratified expression groups.

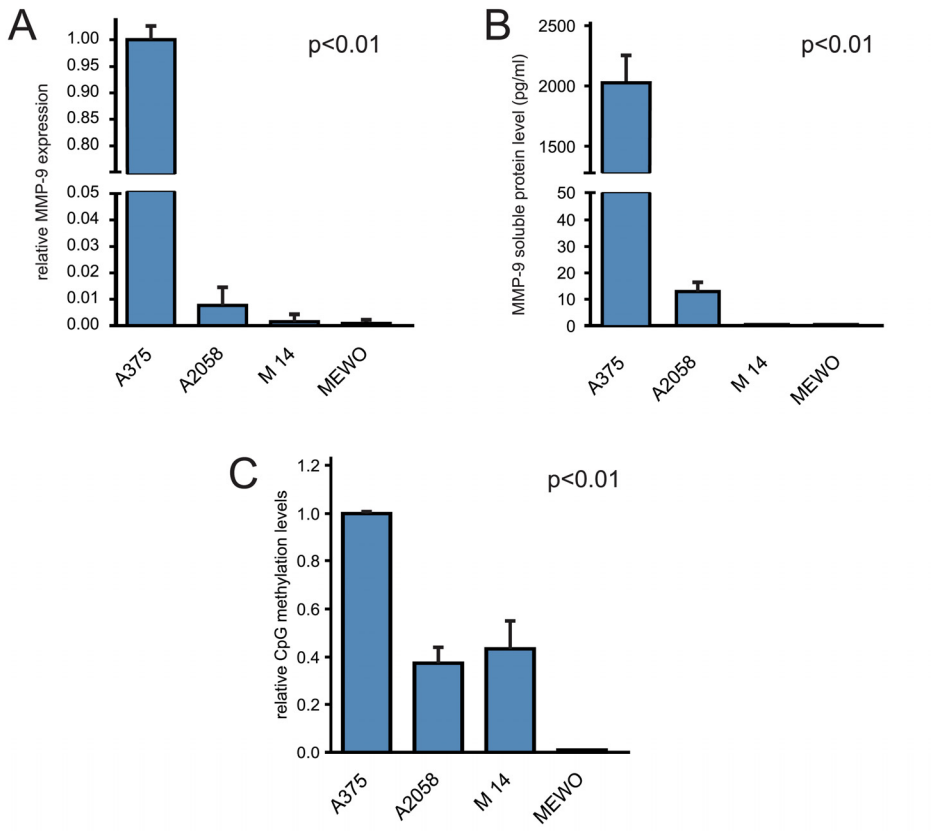

Figure 4. Correlation of MMP-9 CpG-2 hotspot with MMP-9 expression in melanoma cell lines. (**A**) RT-qPCR analysis of MMP-9 transcription levels. (**B**) ELISA determination of released MMP-9 in cell medium supernatant. (**C**) Methylation analysis of MMP9 CpG-2 hotspot in melanoma cell lines by MSRE assay. One-way ANOVA test was performed to analyze statistical significance.

DISCUSSION

Despite recent advances in therapy of metastatic melanoma, the survival rate of patients with melanoma is still low [12,13,14]. The identification of specific prognostic markers suitable to recognize aggressive phenotype in melanoma may improve patient clinical outcome [15].

To our best knowledge, this is the first report describing the intragenic methylation as an additional potential molecular mechanism responsible for the *MMP9* upregulation in cancer. The degradation of pericellular and stromal compartments, mainly mediated by MMP-9, is an essential process during melanoma invasion and migration [3,16]. *MMP9* transcription is strictly regulated by several cytokines and cell/cell or cell/matrix interactions, furthermore the cleavage of proMMP-9 is required for the full proteolytic activity [5,17]. The activation of MMP-9 in cancer has been associated with tumor growth and tumor spreading [18]. Notably, Rangaswami [19] described that MMP-9 is activated in melanoma [19]. The abnormal expression of MMP-9, occurring in cancer cells, may be sustained by hypomethylation or genomic alterations of its promoter [7,11]. All these observations suggested the rational to study MMP-9 in cancer.

Here, we proposed that the intragenic DNA methylation could affect MMP-9 expression. This hypothesis was supported by Singer *et al.* [10]. The authors showed that the intragenic methylation was positively correlated to the gene expression and negatively correlated with the majority of histone modifications involved in gene silencing. Mechanically, the intragenic methylation may affect the transcription elongation, intragenic activation (enhancer) and alternative splicing of several genes [10].

On these bases, we first performed computational analysis to assess the methylation patterns of *MMP9* gene in melanoma samples according to mRNA expression. Such analysis revealed that hypermethylation was observed at the CpG-2 intragenic region in the group with higher MMP-9 expression levels. Accordingly, our in vitro experiments demonstrated that *MMP9* CpG-2 methylation hotspot was correlated with higher transcript and protein levels of MMP-9 in melanoma cell lines. Then, the intervention of epigenetic modifications may be associated with MMP-9 overexpression.

Our results further underline that tumor DNA appears to be the best source to identify the molecular signature of tumor for each patient. The recent advances in the field of biotechnology allow the use of the circulating tumor DNA for the identification of molecular abnormalities, giving a dynamic view of such molecular modifications to evaluate treatment efficacy and patient follow-up [20,21,22]. Among these abnormalities, we might include the *MMP9* intragenic methylation hotspot that is responsible of the MMP-9 overexpression.

Overall, the results of the present study support the notion that *MMP9* intragenic hypermethylation is associated with MMP-9 overexpression that in turn plays a role in cancer development and progression. Furthermore, our data are in agreement with previous studies in which DNA methylation were identified as prognostic markers in cancer [23,24,25,26]. Finally, the increased levels of MMP-9, when associated with such intragenic methylation hotspot, may predict a malignant phenotype.

MATERIALS AND METHODS

Computational identification of CpG islands and methylation status of *MMP9* gene. The CpG islands of *MMP9* gene were identified by computational approaches available on UCSC Genome browser (https://genome.ucsc.edu) (Table S1 and Figure 1A). This tool shows the genomic region satisfying the following conditions: CG content greater than or equal to 50%, length greater than 200 bp and ratio is greater than 0.6 of observed number of CG dinucleotides to the expected number on the basis of the number of Gs and Cs in the segment [27].

Moreover, computational analysis of CpG methylation of *MMP9* locus were explored using ENCODE DNA Methylation by Reduced Representation Bisulfite Sequencing (RRBS) Tracks developed by Encyclopedia of DNA Elements, available on UCSC Genome browser (Figure 1B). This track reports the percentage of DNA fragments that exhibit methylation at specific CpG dinucleotides. DNA methylation status was assayed using RRBS. Briefly, Genomic DNA, extracted from several cell lines, was digested with the methyl-insensitive restriction enzyme MspI. After purification, the small genomic DNA fragments were used to construct an Illumina sequencing library. This genomic library was treated with sodium bisulfite and amplified by PCR to convert every unmethylated cytosine in a thymidine while methylated cytosines were protected from bisulfite conversion. The sequenced fragments were aligned to the reference genome sequence to calculate the percentage of sequence that showed methylated CpG dinucleotides [28].

Melanoma dataset analysis for MMP-9 mRNA expression and methylation. Publicly available Gene Expression Omnibus (GEO) datasets of melanoma were analyzed to evaluate the association between MMP-9 mRNA expression and methylation status of *MMP9* locus. Only datasets with both gene expression and DNA methylation profiling by genome tiling array were considered for the analysis. According to these criteria only the dataset GSE31879 was suitable for the present study. Expression data were obtained using Affymetrix Human Genome U133 Plus 2.0 while methylation profiling data were evaluated by Human DNA Methylation 3x720K CpG Island Plus RefSeq Promoter Array platform (Roche NimbleGen, Inc. - Germany).

In this dataset only 10 of 11 melanoma specimens and 3 of 5 melanocyte cells samples exhibited both mRNA expression levels and DNA methylation status. Melanoma samples were stratified into 3 groups: low (below 30th percentile), medium (between 30th and 70th percentile) and high (above 70th percentile) according to MMP-9 mRNA expression (Figure S1). Methylation-sensitivity probes specific for *MMP9* gene, were grouped into Promoter, Intron-1, CpG-1, CpG-2, CpG-3 and CpG-4 regions according to alignment position of each probe with the promoter, the first intron and the previously named CpG islands of *MMP9* gene (Table S2, Figure 2 and 3).

Cell lines and culture conditions. Melanoma cell lines A375, A2058 and MEWO were obtained from the ATCC (Rockville, MD, USA). M14 cell line was available at the Department of Biomedical and Biotechnological Sciences of the University of Catania. Cells were maintained in a humidified 5% CO_2 incubator at 37°C with RPMI-1640 for A375, A2058 and M14 while EMEM was used for MEWO. Both media were supplemented with 2 mmol/L L-glutamine, 100 IU penicillin and 100 µg/ml streptomycin and 10% fetal bovine serum (FBS). All media and supplements were provided from Lonza (Walkersville, USA).

All cell lines were plated in triplicate into 100 mm cell-culture dishes (Thermo Fisher Scientific Inc., USA) and grown under normal culture conditions to 80% confluency. Supernatants of each cell culture were harvested and centrifugated to remove cellular debris. Adherent cells were washed once and scraped in 1X DPBS (Lonza, Walkersville, USA). Cellular pellets were collected via centrifugation and stored at -80°C.

RT-qPCR analysis. Total cellular RNAs were extracted from cultured cell lines with The PureLink® RNA Mini Kit (Thermo Fisher Scientific Inc., USA) according to the manufacturer's instructions. The concentration and purity of the RNAs were ascertained on a NanoDrop spectrophotometer (Thermo Scientific). Reverse transcription was carried out using M-MLV reverse transcriptase (Invitrogen) and random primers (Invitrogen). SYBR green-based real time PCR was conducted with the Applied Biosystem 7500 Real-Time PCR System using SYBR Green PCR Master Mix (Applied Biosystem, USA). The amplification of *MMP9* and the Phosphoglycerate Kinase 1 (*PGK1*) cDNAs, were performed in triplicate using primers and amplification conditions reported in Table S3. The ddCt relative quantification method was performed to quantify the expression of MMP-9 using PGK-1 signal value as control reference.

ELISA. MMP-9 protein levels were detected in supernatants of each melanoma cell culture using MMP-9 Human ELISA Kit (Invitrogen) according to the datasheet. Briefly, the plate was coated in duplicate with 100 µL of supernatants, standards and controls. The plate was left at RT for 2 hours. After washing four times with wash buffer, 100 µL of streptoavidin-HRP conjugated were added to plate and incubated for 30 min at RT. Then, the plate was washed four times and 100 µL of stabilized chromogen were added to each well. After 30 min incubation, the substrate reaction was stopped with stop solution. Finally, optical density (OD) was measured by Tecan ELISA plate reader (Tecan, Switzerland). The averages of duplicate readings of standards and controls were used to generate the standard curve by linear regression analysis. MMP-9 concentrations were calculated fitting the average of duplicate ODs of each sample with standard curve.

Methylation-specific restriction enzyme assay (MSRE). Methylation-specific restriction enzyme (MSRE) assay is based on use of endonucleases that are not able to cleave methylated-cytosine residues contained in specific consensus sites, leaving methylated DNA intact. Amplification levels of target sequence depend on its content of methylated CpGs, in particular low amplification signal is observed in hypomethylated DNA while higher signal is detected in hypermethylated sequence.

Genomic DNA was extracted from melanoma cell lines using Illustra triplePrep Kit (GE Healthcare, USA) according to manufacturer's instructions. DNA of each sample was digested with restriction enzymes HpaII (New England Biolabs) as explained below.

Each restriction mixture, equally distributed in 0.2 ml reaction tubes, was composed of 50 units of HpaII (5 µL), 5 µL of corresponding 10X REact 8 (New England Biolabs), 1 µg of DNA sample and filled to 50 µL with DNAse free water. Similarly, for each sample the same restriction mixtures without HpaII enzyme were prepared and used as control reference. The methylation insensitive MspI restriction enzyme was used to test the efficiency of MSRE assay.

The restriction reactions and matching controls were incubated at 37°C for 8 hours. Subsequently, 2 µL of Proteinase K (NEB) (20 mg/mL) were added to each tube and placed at 40°C for 30 min, followed by denaturation at 95°C for 10 min. 5 µL of all samples (digested DNA and controls) were subjected to real SYBR green-based real time PCR. The CpG-2 hotspot region, as identified by bioinformatic approaches, was amplified using primers and amplification conditions as shown in table S3. All analyses were performed in triplicate.

Statistics analysis. No additional normalization procedures were applied to data obtained from GSE31879 dataset included in this study. For each MMP-9 expression group, above described, we performed the average of cumulative methylation probe values of the promoter region, of the intron 1 element, and the annotated CpG islands, previously identified in *MMP9* locus. Student's t-Test, one-way ANOVA test and Pearson correlation analysis were performed by R software (www.r-project.org).

Funding

This work was supported by the Lega Italiana per la Lotta contro i Tumori.

Conflict of interest statement

The authors declare no conflict of interest.

REFERENCES

1. Ansieau S, Hinkal G, Thomas C, Bastid J, Puisieux A. Early origin of cancer metastases: dissemination and evolution of premalignant cells. Cell Cycle. 2008; 7:3659-3663.

2. Spagnolo F, Ghiorzo P, Queirolo P. Overcoming resistance to BRAF inhibition in BRAF-mutated metastatic melanoma. Oncotarget. 2014; 5:10206-10221. doi: 10.18632/oncotarget.2602.

3. Shay G, Lynch CC, Fingleton B. Moving targets: Emerging roles for MMPs in cancer progression and metastasis. Matrix Biol. 2015; 44-46:200-206.

4. Huang CY, Tseng KC, Lin MN, Tsai JP, Su CC. Plasma levels of matrix metalloproteinase-2 and -9 in male and female patients with cirrhosis of different aetiologies. J Clin Pathol. 2015; 68:917-922.

5. Chen YJ, Chang LS. NFκB- and AP-1-mediated DNA looping regulates matrix metalloproteinase-9 transcription in TNF-α-treated human leukemia U937 cells. Biochim Biophys Acta. 2015; 1849:1248-1259.

6. Shin SY, Kim JH, Baker A, Lim Y, Lee YH. Transcription factor Egr-1 is essential for maximal matrix metalloproteinase-9 transcription by tumor necrosis factor alpha. Mol Cancer Res. 2010; 8:507-519.

7. Yan C, Boyd DD. Regulation of matrix metalloproteinase gene expression. J Cell Physiol. 2007; 211:19-26.

8. Labrie M, St-Pierre Y. Epigenetic regulation of mmp-9 gene expression. Cell Mol Life Sci. 2013; 70:3109-24.

9. Bedi U, Mishra VK, Wasilewski D, Scheel C, Johnsen SA. Epigenetic plasticity: a central regulator of epithelial-to-mesenchymal transition in cancer. Oncotarget. 2014; 5:2016-2029. doi: 10.18632/oncotarget.1875.

10. Singer M, Kosti I, Pachter L, Mandel-Gutfreund Y. A diverse epigenetic landscape at human exons with implication for expression. Nucleic Acids Res. 2015; 43:3498-3508.

11. Kulis M, Queirós AC, Beekman R, Martín-Subero JI. Intragenic DNA methylation in transcriptional regulation, normal differentiation and cancer. Biochim Biophys Acta. 2013; 1829:1161-1174.

12. Candido S, Rapisarda V, Marconi A, Malaponte G, Bevelacqua V, Gangemi P, Scalisi A, McCubrey JA, Maestro R, Spandidos DA, Fenga C, Libra M. Analysis of the B-RafV600E mutation in cutaneous melanoma patients with occupational sun exposure. Oncol Rep. 2014; 31:107910-82.

13. Russo A, Ficili B, Candido S, Pezzino FM, Guarneri C, Biondi A, Travali S, McCubrey JA, Spandidos DA, Libra M. Emerging targeted therapies for melanoma treatment. Int J Oncol. 2014; 45:516-24.

14. Maira F, Catania A, Candido S, Russo AE, McCubrey JA, Libra M, Malaponte G, Fenga C. Molecular targeted therapy in melanoma: a way to reverse resistance to conventional drugs. Curr Drug Deliv. 2012; 9:17-29.

15. Cheng Y, Lu J, Chen G, Ardekani GS, Rotte A, Martinka M, Xu X, McElwee KJ, Zhang G, Zhou Y. Stage-specific prognostic biomarkers in melanoma. Oncotarget. 2015; 6:4180-4189. doi: 10.18632/oncotarget.2907.

16. Moro N, Mauch C, Zigrino P. Metalloproteinases in melanoma. Eur J Cell Biol. 2014; 93:23-29.

17. Sternlicht MD, Werb Z. How matrix metalloproteinases regulate cell behavior. Annu Rev Cell Dev Biol. 2001; 17:463-516.

18. Mehner C, Hockla A, Miller E, Ran S, Radisky DC, Radisky ES. Tumor cell-produced matrix metalloproteinase 9 (MMP-9) drives malignant progression and metastasis of basal-like triple negative breast cancer. Oncotarget. 2014; 5:2736-2749. doi: 10.18632/oncotarget.1932.

19. Rangaswami H, Bulbule A, Kundu GC. Nuclear factor-inducing kinase plays a crucial role in osteopontin-induced MAPK/IkappaBalpha kinase-dependent nuclear factor kappaB-mediated promatrix metalloproteinase-9 activation. J Biol Chem. 2004; 279:38921382-35.

20. Gray ES, Rizos H, Reid AL, Boyd SC, Pereira MR, Lo J, Tembe V, Freeman J, Lee JH, Scolyer RA, Siew K, Lomma C, Cooper A, Khattak MA, Meniawy TM, Long GV, Carlino MS, Millward M, Ziman M. Circulating tumor DNA to monitor treatment response and detect acquired resistance in patients with metastatic melanoma. Oncotarget. 2015; 6:42008-42018. doi: 10.18632/oncotarget.5788.

21. Janku F, Angenendt P, Tsimberidou AM, Fu S, Naing A, Falchook GS, Hong DS, Holley VR, Cabrilo G, Wheler JJ, Piha-Paul SA, Zinner RG1, Bedikian AY, Overman MJ, Kee BK, Kim KB, Kopetz ES, Luthra R, Diehl F, Meric-Bernstam F, Kurzrock R. Actionable mutations in plasma cell-free DNA in patients with advanced cancers referred for experimental targeted therapies. Oncotarget. 2015; 6:12809-12821. doi: 10.18632/oncotarget.3373.

22. Delyon J, Varna M, Feugeas JP, Sadoux A, Yahiaoui S, Podgorniak MP, Leclert G, Dorval SM, Dumaz N, Janin A, Mourah S, Lebbé C. Validation of a preclinical model for assessment of drug efficacy in melanoma. Oncotarget. 2016; Epub ahead of print. doi: 10.18632/oncotarget.7541.

23. Shinjo K, Kondo Y. Targeting cancer epigenetics: Linking basic biology to clinical medicine. Adv Drug Deliv Rev. Adv Drug Deliv Rev. 2015; 95:56-64.

24. Virani S, Light E, Peterson LA, Sartor MA, Taylor JM, McHugh JB, Wolf GT, Rozek LS; and Investigators of the University of Michigan Head and Neck Specialized Programs of Research Excellence (SPORE) Program. Stability of methylation markers in head and neck squamous cell carcinoma. Head Neck. 2015. [Epub ahead of print]

25. Shan M, Yin H, Li J, Li X, Wang D, Su Y, Niu M, Zhong Z, Wang J, Zhang X, Kang W, Pang D. Detection of aberrant methylation of a six-gene panel in serum DNA for diagnosis of breast cancer. Oncotarget. 2016. [Epub ahead of print]. doi: 10.18632/oncotarget.7608

26. Jones A, Teschendorff AE, Li Q, Hayward JD, Kannan A, Mould T, West J, Zikan M, Cibula D, Fiegl H, Lee SH, Wik E, Hadwin R, Arora R, Lemech C, Turunen H, Pakarinen P, Jacobs IJ, Salvesen HB, Bagchi MK, Bagchi IC, Widschwendter M. Role of DNA methylation and epigenetic silencing of HAND2 in endometrial cancer development. PLoS Med. 2013; 10:e1001551.

27. Gardiner-Garden M, Frommer M. CpG islands in vertebrate genomes. J Mol Biol. 1987; 196:261-282.

28. Meissner A, Mikkelsen TS, Gu H, Wernig M, Hanna J, Sivachenko A, Zhang X, Bernstein BE, Nusbaum C, Jaffe DB et al. Genome-scale DNA methylation maps of pluripotent and differentiated cells. Nature. 2008; 454:766-770.

SUPPLEMENTARY DATA

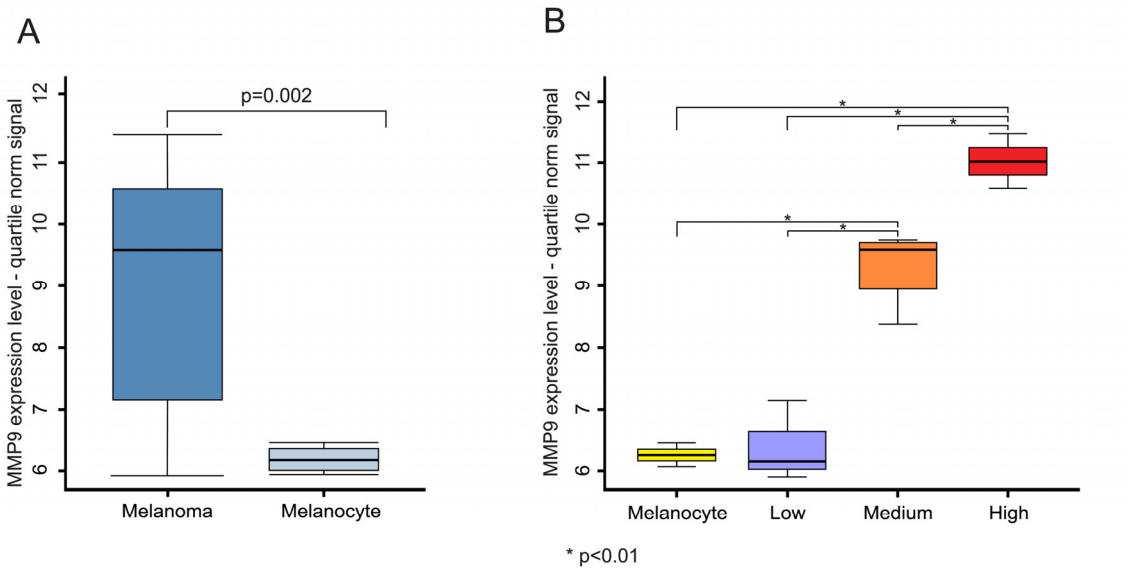

Figure S1. Microarray analysis of MMP-9 expression levels in melanoma samples. (**A**) Differential analysis of MMP-9 expression between melanoma samples and melanocyte controls. (**B**) Statistical analysis among melanoma samples stratified in low, medium and high expression group according the MMP-9 expression levels.

Table S1. CpG islands of MMP-9 gene according to CpG Islands Tracks available in UCSC Genome browser.

Region name	*Chromosome position	Size	CpG count
CpG 1	chr20:46010497-46011349	853	65
CpG 2	chr20:46011650-46012571	922	63
CpG 3	chr20:46013456-46013767	312	24
CpG 4	chr20:46013967-46014472	506	57

*Human Dec. 2013 (GRCh38/hg38) Assembly

Table S2. Pearson Correlation analysis between methylation probset levels and the levels of MMP-9 expression. For each probset, chromosome position, nucleotide sequence and region in which it belongs were reported.

Region	*Chromosome position	Sequence	R	p
Promoter	chr20:46006492-46006543	TCATATTACTCTATGACCTCACATTCCCG AGTCTAGAATCTAGTTCCTCCTG	-0.14	0.5549
Promoter	chr20:46006592-46006641	TTACCTTCAGTGGGTAGCAGGGGACCAG AGGAGAAGCATCCAGGTTTTAT	0.18	0.8355
Promoter	chr20:46006668-46006724	TACCCACTTCTATACCTGGGTCATCACA GTTCCCTGTAAATGGTAATAAAGATGAA A	0.06	0.5903
Promoter	chr20:46006768-46006817	GGATTAACTCGCTCTGTGATCACAGGCA AATTCCTTAACTCTCTGAGCCT	-0.16	0.7741
Promoter	chr20:46006870-46006920	TGGTGAGGATGAAACGAGAGGCTTATAG AGAACTTATTACGGTGCTTGACA	-0.09	0.7255
Promoter	chr20:46006992-46007041	CTGGAAAATGGCAGAGCCGGGATGGAA ATCCAGGACTTCGTGACTGCAAA	-0.11	0.1782
Promoter	chr20:46007090-46007152	AGGAAGTTAATTATCTCCATCTCACAGT CTCATTTATTAGATAAGCATATAAAATG CCTGGCA	0.4	0.0063
Promoter	chr20:46007492-46007542	CAACTTTTTGAGTTGTTAGCAGGTTTTTC CCAAATAGGGCTTTGAAGAAGG	0.71	0.1293
Promoter	chr20:46007592-46007641	GGAGGCTGCTGGTGTGGGAGGCTTGGGA GGGAGGCTTGGCATAAGTGTGA	0.44	0.8936
Promoter	chr20:46007674-46007723	AGGGCTGGAGAACTGAAAGGGCTCCTAT AGATTATTTTCCCCCATATCCT	0.04	0.956
Promoter	chr20:46007788-46007838	TGCAGCTTAGAGCCCAATAACCTGGTTT GGTGATTCCAAGTTAGAATCATG	0.02	0.956
Promoter	chr20:46007992-46008041	GCCCTGAATCTTGGGTCTTGGCCTTAGTA ATTAAAACCAATCACCACCAT	-0.13	0.6784
Promoter	chr20:46008096-46008145	TTTAATCCTCACATCAATTTAGGGACAA AGAGCCCCCCACCCCCCGTTTT	-0.33	0.2704
Promoter	chr20:46008202-46008251	AAGGAAGAGAGTAAAGCCATGTCTGCTG TTTTCTAGAGGCTGCTACTGTC	-0.43	0.1433
Promoter	chr20:46008314-46008363	AGCCTTGCCTAGCAGAGCCCATTCCTTC CGCCCCCAGATGAAGCAGGGAG	-0.13	0.6831
Promoter	chr20:46008398-46008447	AAAAAGAGGACAGAGCCTGGAGTGTGG GGAGGGGTTTGGGGAGGATATCT	-0.41	0.1593
Promoter	chr20:46008502-46008551	TTCAGAAAGAAGTCTCAGGGAGTCTTCC ATCACTTTCCCTTGGCTGACCA	-0.16	0.6093
Promoter	chr20:46008602-46008651	TCCCTCCCTTTCATACAGTTCCCACAAGC TCTGCAGTTTGCAAAACCCTA	-0.33	0.2647
Promoter	chr20:46008692-46008741	TCTTGCCTGACTTGGCAGTGGAGACTGC GGGCAGTGGAGAGAGGAGGAGG	-0.38	0.1972
Promoter	chr20:46008810-46008859	ACACACACACCCTGACCCCTGAGTCAGC ACTTGCCTGTCAAGGAGGGGTG	0.64	0.0187
Promoter	chr20:46008892-46008941	AACAGCAGCTGCAGTCAGACACCTCTGC CCTCACCATGAGCCTCTGGCAG	-0.38	0.1987
Intron 1	chr20:46009008-46009057	CTTGTGCTCTTCCCTGGAGACCTGAGAA CCAATCTCACCGACAGGCAGCT	-0.36	0.2273
Intron 2	chr20:46009108-46009157	GGGTGTTGAGTGTCCCAGAGAGGATGCA GGGCCTCAGAGGAGATGCTTTA	-0.47	0.1054
Intron 3	chr20:46009208-46009257	TTAGGCAGTGGGGGGTCTTGTGGAGGCT TTGAGCAGTGATGGCCAGAAAT	-0.48	0.1008

Intron 4	chr20:46009317-46009366	GAGGGTTCTGGGGTAAGCATAGGCTGGG AGTGAACAGGGGCAAACCTTAT	-0.5	0.0813
Intron 5	chr20:46009413-46009462	GAGCTGAGGATGTCTAAGGAGGGGAGA TCCCTGGGTGGTCAGAAAGCACT	-0.63	0.0216
1CpG	chr20:46010496-46010545	TCGGAAGACTTGCCGCGGGCGGTGATTG ACGACGCCTTTGCCCGCGCCTT	0.53	0.0601
1°CpG	chr20:46010604-46010653	GACATCGTCATCCAGTTTGGTGTCGCGG GTGAGAACGTGAGGAGGGAAAA	0.38	0.195
1°CpG	chr20:46010720-46010769	GGCTTCCTCTTGCCTGCCCGCGCTGCCCT GGCTTATACGGCCCCTCCTGC	0.42	0.1579
1°CpG	chr20:46010804-46010853	AGAGCTTCGCGCAGGCGGGATTTCAGCC CGCACTTATTTCGGAGCCCTTG	0.51	0.078
1°CpG	chr20:46010912-46010961	GTTTCTTCAGAGCACGGAGACGGGTATC CCTTCGACGGGAAGGACGGGCT	0.12	0.7051
1°CpG	chr20:46011008-46011057	CATTTCGACGATGACGAGTTGTGGTCCC TGGGCAAGGGCGTCGGTGAGAT	0.03	0.9121
1°CpG	chr20:46011116-46011165	TAACTCCGGTCCCCCCTCCTCCTGCAGTG GTTCCAACTCGGTTTGGAAAC	0.04	0.8886
1°CpG	chr20:46011216-46011265	CTCTGCCTGCACCACCGACGGTCGCTCC GACGGCTTGCCCTGGTGCAGTA	0.47	0.1047
1°CpG	chr20:46011296-46011345	TTGGCTTCTGCCCCAGCGAGAGTGAGTG AGGGGGCTCGCCGAGGGCTGGG	0.12	0.6945
2°CpG	chr20:46011672-46011721	TCCGACGGCTACCGCTGGTGCGCCACCA CCGCCAACTACGACCGGGACAA	0.6	0.0313
2°CpG	chr20:46011750-46011799	ACCTCCACCCTGTCTACCAGGTTCAGCC CCGCCCTCTCATCATGTATTGG	0.5	0.0789
2°CpG	chr20:46011868-46011917	TGACTCCGCCCACCTACACCACATTTCC ACCACTATCCCTGACTTCCAAT	0.63	0.0215
2°CpG	chr20:46011968-46012017	TCTTCCTTGGTCTGGTGTCCCAGGCACCG CCCACGGGTCTAGCCTCTTCT	0.61	0.0265
2°CpG	chr20:46012056-46012105	GTTTAGCTCCCTGTCGGGTCGGCCCCTG ACTCCTTATTGGACTCATCCAT	0.67	0.0114
2°CpG	chr20:46012174-46012223	GCTGTGCGTCTTCCCCTTCACTTTCCTGG GTAAGGAGTACTCGACCTGTA	0.89	0
2°CpG	chr20:46012250-46012299	CTCTGGTGCGCTACCACCTCGAACTTTG ACAGCGACAAGAAGTGGGGCTT	0.87	0.0001
2°CpG	chr20:46012374-46012423	CAGGGCTGGGGGCTCGGCCCGGCGCTCA CGTCTCAGGCTCCCTCTCCCTC	0.69	0.0089
2°CpG	chr20:46012472-46012521	TGGGCTTAGATCATTCCTCAGTGCCGGA GGCGCTCATGTACCCTATGTAC	0.67	0.0127
2°CpG	chr20:46012550-46012599	AGGACGACGTGAATGGCATCCGGCACCT CTATGGTGAGGCAGGGGCAGGG	0.8	0.0009
3°CpG	chr20:46013265-46013314	TGAACCTGAGCCACGGCCTCCAACCACC ACCACACCGCAGCCCACGGCTC	-0.05	0.8632
3°CpG	chr20:46013379-46013428	CACAGGTCCCCCCTCAGCTGGCCCCACA GGTCCCCCCACTGCTGGCCCTT	0	0.9947
3°CpG	chr20:46013461-46013510	GACGATGCCTGCAACGTGAACATCTTCG ACGCCATCGCGGAGATTGGGAA	0.21	0.5001
3°CpG	chr20:46013585-46013634	GCCCGTCCCTTCCCGCCCACTGGCCCTGT GTCCAAGGCTTAGAGCCCGTC	0.19	0.5286
3°CpG	chr20:46013685-46013734	GGGAGCCGGCCGCAGGGCCCCTTCCTTA TCGCCGACAAGTGGCCCGCGCT	-0.24	0.4315
3°CpG	chr20:46013763-46013812	GAGCGGCTCTCCAAGAAGCTTTTCTTCTT CTCTGGTTAGTTACCTACTTT	0.06	0.8503
3°CpG	chr20:46013862-46013911	ATCGATAACCCACGAAACGTCTTGTGCG TTTTAGAAAAATACGCCCCCTG	0.02	0.9419

4°CpG	chr20:46013962-46014011	CTCCACGCCCTCGCGTCGCTCTACCCAG CGCCTCTGCCCCTGGGTTGCAG	0.32	0.2922
4°CpG	chr20:46014066-46014115	TCTAGGAGTACGTGCTCCCTCTGCGCCC CCAAACCGACGTGACCCTCCTC	0.08	0.8071
4°CpG	chr20:46014164-46014213	CCCGAGGCGTCTGGACAAGCTGGGCCTG GGAGCCGACGTGGCCCAGGTGA	0.36	0.2217
4°CpG	chr20:46014286-46014335	CGCGGCCGCCGGCAGGGGGAGCCCGGG CGCCGTCGGTCCGTCCGCTAGCC	-0.17	0.5722
4°CpG	chr20:46014372-46014421	TTCGACGTGAAGGCGCAGATGGTGGATC CCCGGAGCGCCAGCGAGGTGGA	0.17	0.5791
4°CpG	chr20:46014482-46014531	CTGAGGAGGATCCCTTCGTGAGACACCA CACTAAGCTCCTCTTAGTGAGT	0.05	0.8791
4°CpG	chr20:46014586-46014635	AGCACAGACAAGATCCCAGCAGAGGCA GAGGCCTTCTCCAGGTCATTTAG	-0.06	0.836

*Human Dec. 2013 (GRCh38/hg38) Assembly

Table S3. Primers and real time amplification conditions.

RT-qPCR:		
MMP-9 forward	5'-GAACCAATCTCACCGACAGG-3'	94°C for 10 min, followed by forty cycles of 94°C for 15 s, 64°C for 40 s and 72°C for 1 min.
MMP-9 reverse	5'-CCACAACTCGTCATCGTCG-3'	
PGK-1 forward	5'-TTAAAGGGAAGCGGGTCGTT-3'	
PGK-1 reverse	5'-CAGGCATGGGCACACCAT-3'	
MSRE-qPCR:		
CpG 2 hotspot forward	5'- GTGCGCTACCACCTCGAACT-3'	94°C for 10 min, followed by forty cycles of 94°C for 15 s, 62°C for 20 s and 72°C for 40 s.
CpG 2 hotspot reverse	5'-AGGCTCTGCTTCCAGACAGACG-3'	